

Optical Engineering

OpticalEngineering.SPIEDigitalLibrary.org

Polarization-selective uncooled infrared sensor with asymmetric two- dimensional plasmonic absorber

Shinpei Ogawa
Kyohei Masuda
Yousuke Takagawa
Masafumi Kimata

Polarization-selective uncooled infrared sensor with asymmetric two-dimensional plasmonic absorber

Shinpei Ogawa,^{a,*} Kyohei Masuda,^b Yousuke Takagawa,^b and Masafumi Kimata^{b,*}

^aMitsubishi Electric Corporation, Advanced Technology R&D Center, 8-1-1 Tsukaguchi-Honmachi, Amagasaki, Hyogo 661-8661, Japan

^bRitsumeikan University, College of Science and Engineering, 1-1-1 Noji-higashi, Kusatsu, Shiga 525-8577, Japan

Abstract. A polarization-selective uncooled infrared (IR) sensor was developed based on an asymmetric two-dimensional plasmonic absorber (2-D PLA). The 2-D PLA has an Au-based 2-D periodic dimple structure, where photons can be manipulated by spoof surface plasmon polaritons. Asymmetry was introduced into the 2-D PLA to realize a polarization selective function. Numerical investigations demonstrate that a 2-D PLA with ellipsoidal dimples (2-D PLA-E) gives rise to polarization-dependent absorption properties due to the asymmetric dimple shape. A microelectromechanical systems-based uncooled IR sensor was fabricated using a 2-D PLA-E through complementary metal oxide semiconductor (CMOS) and micromachining techniques. The 2-D PLA-E was formed with an Au layer sputtered on a SiO₂ layer with ellipsoidal holes. The dependence of the responsivity on the polarization indicates that the responsivity is selectively enhanced according to the polarization and the asymmetry of the ellipsoids. The results provide direct evidence that a polarization-selective uncooled IR sensor can be realized simply by the introduction of asymmetry to the surface structure of the 2-D PLA, without the need for a polarizer or optical resonant structures. In addition, a pixel array where each pixel has a different detection polarization could be developed for polarimetric imaging using standard CMOS and micromachining techniques.

© The Authors. Published by SPIE under a Creative Commons Attribution 3.0 Unported License. Distribution or reproduction of this work in whole or in part requires full attribution of the original publication, including its DOI. [DOI: [10.1117/1.OE.53.10.107110](https://doi.org/10.1117/1.OE.53.10.107110)]

Keywords: polarization-selective; plasmonics; metamaterial; uncooled; infrared sensors.

Paper 141182P received Jul. 28, 2014; revised manuscript received Sep. 25, 2014; accepted for publication Sep. 29, 2014; published online Oct. 28, 2014.

1 Introduction

Infrared (IR) sensors are used to detect objects that emit IR radiation, and images can be constructed based on the IR intensity using pixel-array structures. Uncooled IR image sensors with a microelectromechanical (MEMS) system-based pixel structure possess significant advantages, such as low cost, ease of manufacture, and a wide range of applications.¹⁻³

The authors are developing uncooled IR sensors with advanced functions to exploit their potential and expand their applications. For example, wavelength-selective uncooled IR sensors have recently been realized using a two-dimensional plasmonic absorber (2-D PLA) with wavelength selectivity in the middle and long wavelength IR regions.⁴⁻⁶ The 2-D PLA has a periodic array of circular dimples on its surface, where photons can be manipulated by spoof surface plasmon polaritons.⁷⁻⁹ The detection wavelength is determined by the reciprocal lattice vector of the 2-D PLA.¹⁰ The 2-D PLA has an advantage in that the detection wavelength can be controlled simply by the surface structure and without the need for filters,^{11,12} multilayer structures,^{13,14} or optical resonant structures.^{15,16} Such wavelength-selective uncooled IR sensors that employ plasmonics will contribute to the development of novel multicolor imaging for IR sensors.

Light has certain characteristics such as intensity, wavelength, polarization, and coherence, of which intensity and wavelength have been fully utilized for wavelength-selective

uncooled IR sensors. As the next step, we have developed a polarization discrimination function for advanced uncooled IR sensors. Artificial objects, such as vehicles, buildings, roads, and agricultural fields, change the polarization state of the electromagnetic field reflected or emitted from their surfaces. Therefore, human influences can be distinguished from the natural environment on the Earth by polarimetric sensing.¹⁷⁻²⁰

A pixel array in which each pixel has a different absorption polarization angle could be used to realize polarimetric imaging at various IR wavelengths, which would provide a significant advantage for the detection of human influence in the environment. Therefore, polarization selectivity is a promising function for advanced IR sensing. A polarizer is often used to achieve polarimetric imaging;^{11,21} however, polarizers are very sensitive to the setting angle of the detector, which can cause optical loss, thus a rotating mechanical system is sometimes required. The attachment of such external optical systems requires additional space and increases the cost. Therefore, such approaches have difficulty with the integration of different pixels in an array for polarimetric imaging.

We have applied plasmonics to address this challenge. Plasmonics is a rapidly growing field of optical physics by which a metal surface structure provides the means for the manipulation of photons.^{22,23} We have previously reported that an Au-based 2-D concave structure can be used as a wavelength-selective absorber.^{4,5} However, the 2-D PLAs that have been developed have no polarization dependence. Asymmetry can be introduced to discriminate the polarization angle of the incident light. Thus, structural asymmetry is used to realize polarization-selective uncooled IR sensors

*Address all correspondence to: Shinpei Ogawa, E-mail: Ogawa.Shimpei@eb.MitsubishiElectric.co.jp; Masafumi Kimata, E-mail: kimata@se.ritsumeik.ac.jp

based on an asymmetric 2-D PLA. We have recently reported that 2-D PLAs with elliptical dimples can produce polarization dependence.²⁴ However, the detailed effect of the asymmetric shape of the elliptical dimples has not yet been reported. Thus, in this study, we provide a detailed report on the polarization selectivity of 2-D PLAs with elliptical dimples.

2 Design

Our previous 2-D PLAs have symmetric lattice structures of circular dimples, such as square^{4,5} and triangular¹⁰ lattices, which provide no polarization dependence. Therefore, asymmetry was introduced to the 2-D PLA to realize polarization selectivity by changing the shape of the PLA dimples from circular to elliptical. The absorption properties of a 2-D PLA with ellipsoidal dimples (2-D PLA-E) indicate polarization dependence due to the asymmetric shape of the ellipse. Figure 1(a) shows a schematic illustration of the Au-based 2-D PLA-E used for the uncooled IR sensor and the definition of the polarization angle (θ) of the electrical field (E)

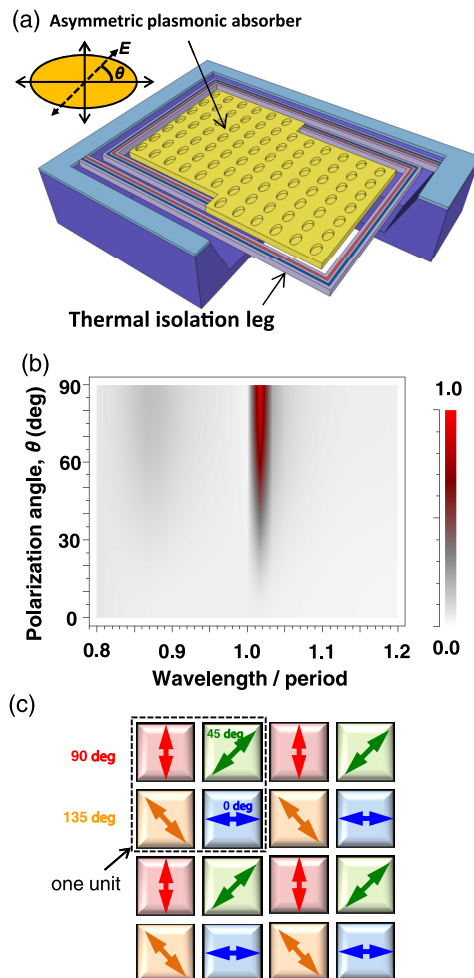


Fig. 1 (a) Schematic diagram of the uncooled IR sensor (thermopile) with Au-based two-dimensional plasmonic absorber (2-D PLA) having ellipsoidal dimples, and definition of the electric field polarization angle to the axis of the ellipsoid. (b) Calculated polarization dependence for the 2-D PLA-E. (c) Concept of a pixel array with various 2-D PLA-Es for polarimetric imaging.

with respect to the ellipse. Absorption is controlled by the filling factor, which is defined as the ratio between the diameter and the period of the dimples on the 2-D PLAs.⁶ The 2-D PLA-E has a periodic array of ellipsoidal dimples on its surface, where the ellipsoid shape introduces an asymmetric filling factor according to the major and the minor axes. Absorption can be selected according to these two axes to achieve polarization dependence.

Figure 1(b) shows the calculated polarization dependence for the absorption of the Au-based 2-D PLA-E with a fixed dimple period (P) of $6.0 \mu\text{m}$, a major axis of $3.0 \mu\text{m}$, a minor axis of $1.5 \mu\text{m}$, and a depth of $1.0 \mu\text{m}$ for comparison with the 2-D PLA having circular dimples.^{4,5} The wavelength was normalized according to P . The strong polarization dependence of the absorption is evident according to θ . When E is vertical to the major axis ($\theta = 90 \text{ deg}$), sufficient absorption is obtained; however, when E is parallel to the major axis ($\theta = 0 \text{ deg}$), there is no absorption. The absorption increases with to the increase of θ , which satisfies the requirements for an uncooled wideband IR sensor with a polarization-selective function. Thus, theoretical calculations demonstrated that the elliptical shape produces polarization dependence.

Figure 1(c) shows the concept of the array structure for 2-D PLA-Es with polarization discrimination. One unit consists of four pixels and 2-D PLA-Es when different absorptions at θ of 0, 45, 90, and 135 deg are employed. Polarimetric imaging can thus be realized by introducing asymmetry to the surface structure.

3 Sensor Fabrication

A MEMS-based uncooled IR sensor with 2-D PLA-Es was developed. The 2-D PLA-Es are fabricated by forming an Au layer on a perforated SiO_2 substrate. Figure 2 shows the procedure used to fabricate the MEMS-based thermopile with a 2-D PLA-E. (a) The devices are fabricated on 6-in. p-type Si (100) substrates using a standard complementary metal oxide semiconductor (CMOS) process. The thermocouples consist of a series of p- and n-type polycrystalline Si regions, of which the resistivity is controlled by ion implantation. An Al layer is formed as a backside reflective layer under the absorber area. Etching holes for bulk micromachining are formed by reactive-ion etching (RIE). A $1.5\text{-}\mu\text{m}$ -thick SiO_2 layer is formed on the absorber area. (b) The periodic ellipsoidal dimple structures are then formed only on the SiO_2 layer of the IR absorber area by RIE. (c) $50/250\text{-nm}$ -thick Cr/Au layers are sputtered, where the Cr layer acts as an adhesion layer between SiO_2 and Au. The 250-nm -thick Au layer is sufficiently thicker than the skin depth in the IR wavelength region.²⁵ Incident IR rays cannot penetrate the Au film, so that absorption by SiO_2 beneath the Au layer is negligible.⁵ The Cr/Au layers are selectively etched using a wet etchant to reveal etching holes covered by the sputtered layers. Scanning electron microscopy (SEM) observation confirmed that the Cr/Au layers were uniformly coated on both the bottom and side walls of the etched holes and the concave Au structures were completed. (d) The wafers are diced into chips. Si is anisotropically etched through the etching holes using tetramethylammonium hydroxide (TMAH). The cavity under the IR absorber area is then formed, which results in the completion of a thermally isolated freestanding structure on which the 2-D PLA-E

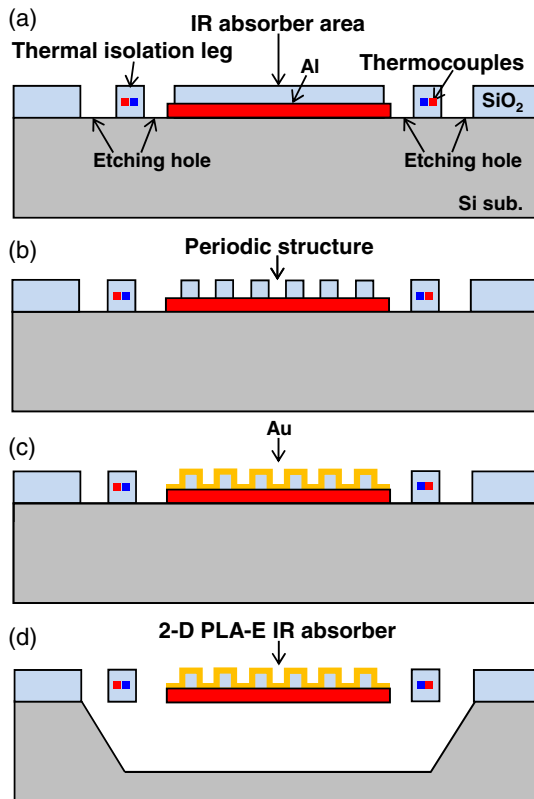


Fig. 2 Schematic diagram of the procedure used to fabricate the microelectromechanical system (MEMS)-based thermopile with 2-D PLA-E. (a) Devices are formed on the surface of a SiO₂/Si wafer by a standard complementary metal oxide semiconductor process. Etching holes are formed by reactive-ion etching. (b) The periodic hole structures are formed on SiO₂ using a dry etching process. (c) Cr/Au layers are sputtered on the perforated SiO₂/Si substrate. (d) The thermally isolated freestanding structure is completed by bulk micromachining.

absorber is formed. The backside and edge of the 2-D PLA-E was coated with Au and Al to prevent absorption by SiO₂.

Figure 3(a) shows an SEM image of one of the developed thermopiles with the 2-D PLA-E. The detector area (300 × 200 μm²) is surrounded by long thermal isolation legs to reduce thermal conductance. Various sensors with different 2-D PLA-E structures were fabricated on the same wafer. The length of the major axis, the period and the depth of the dimples were fixed at 4.0, 5.0, and 1.5 μm for all sensors, respectively, considering the resolution limit of the photolithography system employed. The length of the minor axis was changed and the ellipticity was defined as the ratio of the minor axis length to that of the major axis of the ellipsoid. The respective minor axis lengths of the ellipsoids and the ellipticity were (i) 4.0 μm and 100%, (ii) 3.0 μm and 75%, (iii) 2.5 μm and 62.5%, (iv) 2.0 μm and 50%, and (v) 1.5 μm and 37.5%. Sensor (i) has circular dimples and acts as a reference for comparison. Figure 3(b) shows a magnified SEM image of the 2-D PLA-E sensor (iv) surface, and Fig. 3(c) shows a schematic diagram of the 2-D PLA-E. The top surface of the Au layer acts as an absorption layer. The bottom Al layer prevents backside absorption by the SiO₂ substrate.

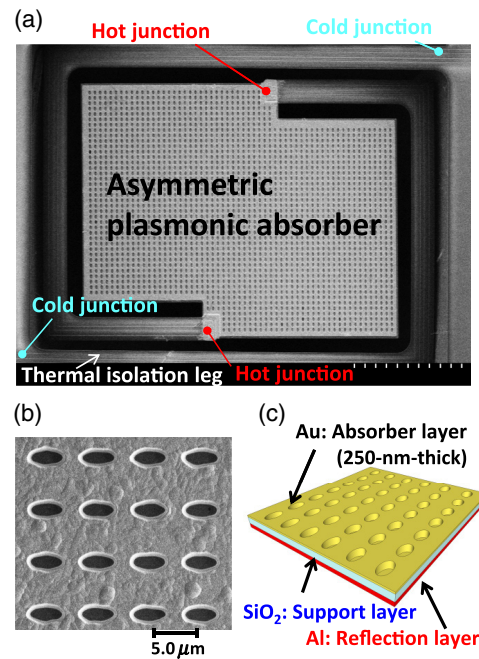


Fig. 3 (a) Scanning electron microscopy (SEM) image of the MEMS-based thermopile with 2-D PLA-E developed in this study. (b) Magnified SEM images of the 2-D PLA-E of sensor (iv). (c) Schematic diagram of the 2-D PLA-E.

4 Measurements

Figure 4 shows a schematic diagram of the experimental setup used to measure the polarization dependence of the 2-D PLA-E. The sensors were set in a vacuum chamber with a BaF₂ window under a pressure of 1 Pa to prevent thermal conduction loss through the atmosphere. IR radiation from a blackbody was irradiated to the sample through narrow bandpass filters for selection of the evaluation wavelengths. The typical full width at half maximum was 80 nm. A polarizer was set in front of the BaF₂ window and a pin-hole was used to restrict the incident light to the 2-D PLA. The polarization angle was defined as shown in Fig. 1(b).

Figure 5 shows the normalized responsivity of sensors (i) to (v) for θ = 0 deg and 90 deg. The responsivity was normalized with respect to the responsivity peak of each sensor

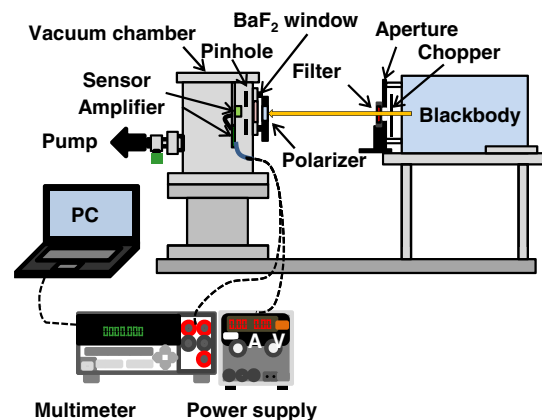


Fig. 4 Schematic diagram of experimental setup used for polarization dependence measurements.

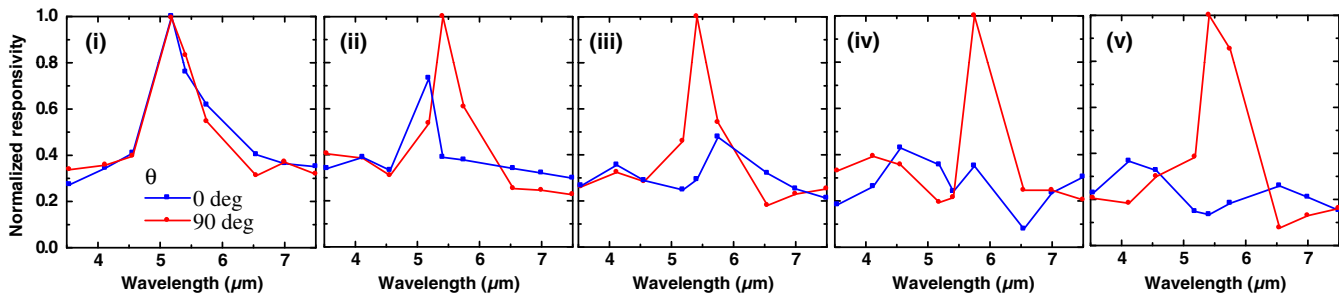


Fig. 5 Measured polarization dependence of the spectral responsivity at $\theta = 0$ deg and 90 deg for sensors (i) to (v).

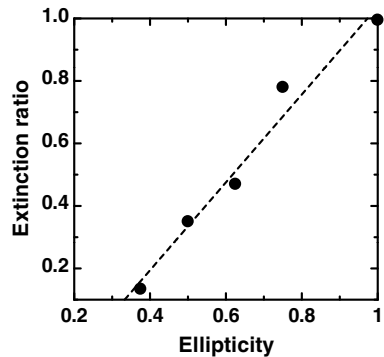


Fig. 6 Extinction ratio as a function of the ellipticity.

to investigate the polarization dependence according to the ellipticity. Sensor (i) with circular dimples has no polarization dependence due to its symmetry. When the incident polarization is vertical to the major axis ($\theta = 90$ deg), the responsivity is clearly enhanced for sensors (ii) to (v). In contrast, the responsivity for parallel polarization ($\theta = 0$ deg) was clearly suppressed according to the decrease of the ellipticity. The measured polarization properties agree well with the calculated results, as shown in Fig. 1(b). Thus, the responsivity is selectively enhanced according to the asymmetric shape of the ellipsoids.

Figure 6 shows the relation between the extinction ratio and the ellipticity. The extinction ratio is defined as the ratio of responsivity of the electric field at $\theta = 0$ deg to that at $\theta = 90$ deg. The responsivity at $\theta = 90$ deg for the extinction ratio was adopted as the peak wavelength. The responsivity at $\theta = 0$ deg was adopted as the peak wavelength for sensors (i) to (iii) and the wavelength corresponding to the peak at $\theta = 90$ deg was adopted for sensors (iv) and (v), due to the lack of a clear peak at the main detection wavelength. Figure 6 shows that the extinction ratio decreased with the ellipticity.

5 Conclusions

A MEMS-based uncooled IR sensor with 2-D PLA-Es was developed using standard CMOS and micromachining techniques. The polarization dependence of the responsivity demonstrates that the enhancement of the selective responsivity according to the polarization angle was successfully achieved and that polarization dependence can be controlled simply with the ellipticity. These results are direct evidence that a polarization-selective uncooled IR sensor can be realized simply by the introduction of asymmetry to the 2-D

PLA surface structure, without the need for polarizers or filters. Control of the detection polarization using asymmetric PLAs could be applied to other types of thermal IR sensors, such as bolometers and silicon-on-insulator diodes.²⁶ The results obtained here will contribute to the development of novel polarimetric imaging for IR sensors.

Acknowledgments

The authors thank Mitsuharu Uetsuki, Daisuke Fujisawa, Masashi Ueno, Tetsuya Satake, Katsuhiko Tsujino and Tetsuji Sorita of the Advanced Technology R&D Center of Mitsubishi Electric Corporation for helpful support.

References

1. P. W. Kruse, *Uncooled Thermal Imaging Arrays, Systems, and Applications*, SPIE, Bellingham, Washington (2001).
2. M. Vollmer and K.-P. Mollmann, *Infrared Thermal Imaging: Fundamentals, Research and Applications*, Wiley-VCH, Weinheim (2010).
3. M. Kimata, "Trends in small-format infrared array sensors," in *2013 IEEE Proc. Sensors*, pp. 1–4, IEEE (2013).
4. S. Ogawa et al., "Wavelength selective uncooled infrared sensor by plasmonics," *Appl. Phys. Lett.* **100**(2), 021111 (2012).
5. S. Ogawa et al., "Wavelength selective wideband uncooled infrared sensor using a two-dimensional plasmonic absorber," *Opt. Eng.* **52**(12), 127104 (2013).
6. K. Masuda et al., "Optimization of two-dimensional plasmonic absorbers based on a metamaterial and cylindrical cavity model approach for high-responsivity wavelength-selective uncooled infrared sensors," *Sens. Mater.* **26**(4), 215–223 (2014).
7. J. B. Pendry, L. Martín-Moreno, and F. J. Garcia-Vidal, "Mimicking surface plasmons with structured surfaces," *Science* **305**(5685), 847–848 (2004).
8. F. J. Garcia-Vidal, L. Martín-Moreno, and J. B. Pendry, "Surfaces with holes in them: new plasmonic metamaterials," *J. Optic. A: Pure Appl. Opt.* **7**(2), 5 (2005).
9. R. Stanley, "Plasmonics in the mid-infrared," *Nat. Photonics* **6**(7), 3 (2012).
10. S. Ogawa et al., "Wavelength selective uncooled infrared sensor using triangular-lattice plasmonic absorbers," in *2013 Int. Conf. on Proc. Optical MEMS and Nanophotonics (OMN)*, pp. 61–62, IEEE (2013).
11. R. Haïdar et al., "Free-standing subwavelength metallic gratings for snapshot multispectral imaging," *Appl. Phys. Lett.* **96**(22), 221104 (2010).
12. Y. Ohtera and H. Yamada, "Photonic crystals for the application to spectrometers and wavelength filters," *IEICE Elec. Exp.* **10**(8), 20132001 (2013).
13. T. Maier and H. Brueckl, "Multispectral microbolometers for the midinfrared," *Opt. Lett.* **35**(22), 3766–3768 (2010).
14. N. Landy et al., "Perfect metamaterial absorber," *Phys. Rev. Lett.* **100**(20), 207402 (2008).
15. S. W. Han et al., "Design of infrared wavelength-selective microbolometers using planar multimode detectors," *Electron. Lett.* **40**(22), 1410–1411 (2004).
16. R. P. Shea, A. S. Gawarikar, and J. J. Talghader, "Midwave thermal infrared detection using semiconductor selective absorption," *Opt. Exp.* **18**(22), 22833–22841 (2010).
17. J. R. Schott, *Fundamentals of Polarimetric Remote Sensing*, SPIE, Bellingham, Washington (2009).
18. J. S. Tyo et al., "Review of passive imaging polarimetry for remote sensing applications," *Appl. Opt.* **45**(22), 5453–5469 (2006).

19. J. S. Tyo et al., "The effects of thermal equilibrium and contrast in LWIR polarimetric images," *Opt. Exp.* **15**(23), 15161–15167 (2007).
20. B. M. Ratliff, C. F. LaCasse, and J. S. Tyo, "Interpolation strategies for reducing IFOV artifacts in microgrid polarimeter imagery," *Opt. Exp.* **17**(11), 9112–9125 (2009).
21. G. W. Kamerman et al., "Polarization state imaging in long-wave infrared for object detection," *Proc. SPIE* **8897**, 88970R (2013).
22. D. K. Gramotnev and S. I. Bozhevolnyi, "Plasmonics beyond the diffraction limit," *Nat. Photonics* **4**(2), 83–91 (2010).
23. S. Kawata, "Plasmonics: future outlook," *Jpn. J. Appl. Phys.* **52**(1), 010001 (2013).
24. S. Ogawa et al., "Polarization selective uncooled infrared sensor using an asymmetric two-dimensional plasmonic absorber," *Proc. SPIE* **9070**, 90701T (2014).
25. F. Neubrech et al., "Properties of gold nanoantennas in the infrared," in *Chapter 12 in Nanostructures in Electronics and Photonics*, F. Rahman, Ed., p. 210, World Scientific Publishing Co., Singapore (2008).
26. D. Fujisawa et al., "Two-million-pixel SOI diode uncooled IRFPA with 15 μm pixel pitch," *Proc. SPIE* **8353**, 83531G (2012).

Shinpei Ogawa received his BE, ME, and PhD degrees from the Department of Electronic Science and Engineering, Kyoto University, Japan, in 2000, 2002, and 2005, respectively. He has been with the Advanced Technology R&D Center, Mitsubishi Electric Corporation,

Amagasaki, Japan, since 2005. He works on the development of various MEMS devices, including RF-MEMS switches, inductors, TSV, optical sensors, infrared sensors, and packaging technology. His current research interests are photonic and plasmonic devices integrated with MEMS technology.

Kyohei Masuda received his BE and ME degrees from the College of Science and Engineering, Ritsumeikan University, Japan, in 2012 and 2014, respectively.

Yosuke Takagawa received his BE degree from the College of Science and Engineering, Ritsumeikan University, Japan, in 2013. He is currently working for his ME degree in the College of Science and Engineering, Ritsumeikan University.

Masafumi Kimata received his MS degree from Nagoya University in 1976, and received his PhD degree from Osaka University in 1992. He joined Mitsubishi Electric Corporation in 1976 and retired from Mitsubishi Electric in 2004. Currently, he is a professor of Ristumeikai University, where he continues his research on MEMS-based uncooled infrared focal plane arrays and type-II superlattice infrared focal plane arrays. He is a Fellow of SPIE.